

Glitch Behavior of Pulsars and Contribution from Neutron Star Crust

AVISHEK BASU,¹ PRASANTA CHAR,² RANA NANDI,³ BHAL CHANDRA JOSHI,¹ AND DEBADES BANDYOPADHYAY⁴

¹*National Centre for Radio Astrophysics - Tata Institute of Fundamental Research
NCRA-TIFR, Pune University Campus, Ganeshkhind, Pune, Maharashtra 411007, India*

²*Inter-University Centre for Astronomy and Astrophysics, Post Bag 4, Ganeshkhind, Pune - 411 007, India*

³*Tata Institute of Fundamental Research - Department of Nuclear and Atomic Physics
Homi Bhabha Road, Navy Nagar, Colaba, Mumbai, Maharashtra 400005, India*

⁴*Astroparticle Physics and Cosmology Division
Saha Institute of Nuclear Physics, HBNI
Sector - 1, Block - AF Bidhan nagar, Kolkata- 700064, India*

ABSTRACT

Pulsars are highly magnetized rotating neutron stars with a very stable rotation speed. Irrespective of their stable rotation rate, many pulsars have been observed with the sudden jump in the rotation rate, which is known as pulsar glitch. The glitch phenomena are considered to be an exhibit of superfluidity of neutron matter inside the neutron star's crustal region. The magnitude of such rapid change in rotation rate relative to their stable rotation frequency can quantify the ratio of the moment of inertia of the crustal region to the total moment of inertia of the star also called as the fractional moment of inertia (FMI). In this paper, we have calculated FMI for different masses of the star using six different representative unified equations of state constructed under relativistic mean field framework. We have performed an event-wise comparison of FMI obtained from data with that of theoretically calculated values with and without considering the entrainment effect. It is found that larger glitches can not be explained by crustal FMI alone, even without the entrainment.

Keywords: Equation of state – stars: interiors – stars: rotation – stars: neutron

1. INTRODUCTION

Pulsars are rotating magnetized neutron stars with magnetic field strength of about 10^{12} G. Most pulsars have very stable rotational periods ranging from milliseconds to a few seconds owing to their compact size and large mass. However, some pulsars do show rotational irregularities, such as sudden jumps in the spin frequencies, known as pulsar glitches (Radhakrishnan & Manchester 1969). In the last five decades, 529 glitches have been reported in radio pulsars (Lyne 1992; Shemar & Lyne 1996; Lyne 1996; Lyne et al. 2000; Wang et al. 2000; Krawczyk et al. 2003; Espinoza et al. 2011; Yu et al. 2013; Fuentes et al. 2017). The reported fractional spin-up during a glitch¹ range from 10^{-9} to 33×10^{-6} (Manchester & Hobbs 2011). Pulsars, such as PSR B0833–45, B1046–58, B1338–62 and B1737–30, show glitches with fractional spin-up varying over three orders of magnitude. The glitch events can also be followed by exponential recoveries of rotation rate (Yu et al. 2013).

It is believed that the interior superfluid is responsible for glitches, where the excess angular momentum of pinned component of superfluid is transferred to the crust at a critical lag between the differential rotation of neutron star's superfluid and non-superfluid component (Alpar et al. 1985, 1984). Observations of pulsar glitches and their recoveries provide important probe of the composition and structure of neutron stars (Haskell & Melatos 2015) in terms of the depth from the surface of the star, where glitches originate. Glitches can also help in understanding how the superfluid component of the star is coupled with the observable crust of the star and whether the core of the star participates in the glitch phenomena. We aim to investigate this by comparing theoretical calculations with reported glitch measurements in this work.

One way to achieve this goal is to place constraints on moment of inertia (MoI) of different parts of the neutron star (NS) participating in the glitch phenomena. There exist distinct density regions inside the star, defined by the local density, which changes from $\sim 10^4$ g cm⁻³ to $\sim 10^{14}$ g cm⁻³ from the surface of NS to its

¹ The fractional spin-up is defined as the ratio of increase in rotation rate $\delta\nu$ to rotation rate ν at the time of glitch.

center. The outer most layer (outer-crust) consists of fully ionized nuclei arranged in BCC lattice structure embedded in degenerate electron gas. With increasing density nuclei become more and more neutron-rich (Baym et al. 1971a; R uster et al. 2006; Nandi & Bandyopadhyay 2011). At the density $\sim 10^{11}$ g cm $^{-3}$, the neutron drip point is reached and the inner crust begins. The inner crust is composed of neutron-rich nuclei arranged in a lattice and immersed in a free electron gas as well as a gas of dripped neutrons (Baym et al. 1971b; Negele & Vautherin 1973; Haensel 2001; Nandi et al. 2011), which are expected to be superfluid (Baldo et al. 2005; Sedrakian & Clark 2006; Chamel & Haensel 2008). Beyond the inner crust, the core of the star may consist of superfluid neutrons, superconducting protons and other exotic matter (Ginzburg & Kirzhnits 1964; Baldo et al. 2005; Sauls 1989; Sedrakian & Clark 2006; Page & Reddy 2006; Chamel & Haensel 2008).

Theoretically, MoI of the crust and core components can be estimated by solving the structure equations with a given Equation of State (EoS). In the study of pulsar glitches, mostly non-relativistic EoSs are used (Andersson et al. 2012; Chamel 2013; Ho et al. 2015; Delsate et al. 2016; Li et al. 2016; Pizzochero et al. 2017). On the other hand, EoSs obtained from relativistic mean field (RMF) model that gives a causal description at all densities of NS have been widely used in the literature to study various properties of nuclear matter as well as NS (Glendenning 2000; Dutra et al. 2014; Oertel et al. 2017). Only Piekarewicz et al. (2014), employed RMF EoSs for the NS core to study the glitch phenomena. However, for the inner crust they used a polytropic EoS that interpolates between the neutron-drip density and the crust-core transition density. Since the inner crust contributes more than 99% to the crustal MoI, it is important to have a realistic EoS for the inner crust. In the literature, the inner crust and the core are often treated separately and the corresponding EoSs are matched ‘‘by hand’’ at the crust-core boundary which is also chosen arbitrarily (Glendenning 2000; Read et al. 2009; Fattoyev et al. 2018). The precision in this matching processes can lead to significant differences in the estimation of MoI of different components (Fortin et al. 2016). Therefore, it is necessary to use a unified EoS where EoSs of both the inner crust and the core are calculated from same microscopic theory and as a consequence, the crust-core boundary is automatically determined. In this article, we calculate MoI using unified EoSs derived from different variation of RMF model.

Pinned neutron superfluid provides an angular momentum reservoir as its rotation rate is determined by the areal vortex density, which is constant as long as it is

pinned to the crust. At the same time, the crust continuously slows down due to loss of its angular momentum in particle wind and electromagnetic radiation. At a critical lag in this differentially rotating two-component system, superfluid vortices get unpinned dumping large amount of angular momentum to the crust, which is seen as a spin up in the crustal rotation rate, usually inferred by timing the radio pulse (Alpar et al. 1985, 1984). This implies that the fractional spin-up provides a probe of the extent of angular momentum transfer and hence MoI of the crustal pinned superfluid. The ratio of the MoI of crustal pinned superfluid to that of the rest of the star, referred to as fractional moment of inertia (FMI), can be related to the observed fractional spin-up, allowing a comparison of theoretical estimates with those from observations (Link et al. 1992, 1999; Eya et al. 2017). In this context, it is common practice in the literature (Link et al. 1999; Andersson et al. 2012; Chamel 2013; Ho et al. 2015; Eya et al. 2017) to define a quantity called activity parameter, which is essentially the average of all glitches observed in a time window for a given pulsar. This parameter is then used to estimate the FMI for different pulsars. However, as we are interested in investigating how far the FMI of the crust could explain the observed glitches, it seems more appropriate to use individual glitches instead of the average. Based on calculation of FMI in eight individual Vela pulsar glitches (Alpar et al. 1993), Datta & Alpar (1993) ruled out one out of 19 EoS for this pulsar. With a better constraint on the maximum mass of NS for different EoS and much larger glitch database 25 years later, this question is worthwhile a detailed re-examination. Therefore, in this article, we consider separately each individual glitch cataloged so far (Espinoza et al. 2011) to estimate the FMI.

In this paper, we apply a unified treatment of Equation of State (EoS), obtained in a variety of RMF models, to estimate the fraction of stellar moment of inertia of the crust and compare it to that inferred from reported observations of pulsar glitches. In Section 2, the construction of the EoS is described followed by estimates of relevant MoI using the structure equations in Section 3. We connect these estimates to observables in Section 4 and present our results in Section 5. Discussion of these results and conclusions is presented in Section 6.

2. EQUATION OF STATE

It has been shown (Fortin et al. 2016) that for an unambiguous calculation of NS properties (especially radius and crust thickness) one needs to employ a unified EoS, i.e., the EoS of crust and core should be ob-

tained within the same many-body theory. As the phenomena of glitch are supposed to be very sensitive to the thickness of the crust, we employ only unified EoSs here. We construct the EoSs of the inner crust and core adopting the RMF approach, where the interaction between nucleons is described by the exchange of σ , ω and ρ mesons. For our study, we choose EoSs that represent different variation of the RMF model and also used widely in the literature (Dutra et al. 2014). In particular, we use parameter sets: NL3 (Lalazissis et al. 1997) and GM1 (Glendenning 2000) that include non-linear self-interaction of σ -mesons, TM1 (Sughara & Toki 1994) that has self-interacting terms for both σ and ω mesons, NL3 $\omega\rho$ (Horowitz & Piekarewicz 2001), which contains self-interaction of σ mesons and coupling between ω and ρ mesons, and DDME2 (Lalazissis et al. 2005) and BHBA ϕ (Banik et al. 2014), where coupling parameters are considered to be density dependent. The EoSs of the inner crust along with the crust-core transition density for all parameter sets excluding BHBA ϕ are taken from Grill et al. (2014), whereas the EoSs of core that contains neutrons, protons, electrons and muons are generated by the standard procedure (Glendenning 2000; Dutra et al. 2014). As EoSs of both the crust and the core are described by the same parameter set, they can be joined smoothly at the crust-core boundary without any jump in pressure and density. For the EoS of outer crust, we choose DH EoS (Haensel et al. 2007). The choice of outer crust does not have any significant impact on the observables as the most part of it is determined from the experimentally measured nuclear masses. The unified BHBA ϕ EoS is obtained following Banik et al. (2014). Apart from nucleons and leptons, the core EoS of BHBA ϕ also includes Λ -hyperons, which interact among themselves via the exchange of ϕ mesons. All six EoSs used here give maximum NS masses (M_{\max}) more than $2M_{\odot}$ and are therefore compatible with the constraint of $M_{\max} = 2.01 \pm 0.04M_{\odot}$ obtained from observation (Antoniadis et al. 2013). We use these EoSs to estimate the MoI relevant for the present work.

3. STRUCTURE

The equilibrium structure of a spherically symmetric, non-rotating NS is calculated from the solutions of Tolman-Oppenheimer-Volkoff (TOV) equations given by,

$$\frac{dP(r)}{dr} = -\frac{[\varepsilon(r) + P(r)] [M(r) + 4\pi r^3 P(r)]}{r [r - 2M(r)]} \quad (1)$$

$$\frac{d\nu(r)}{dr} = -\frac{1}{\varepsilon(r) + P(r)} \frac{dP(r)}{dr} \quad (2)$$

$$\frac{dM(r)}{dr} = 4\pi r^2 \varepsilon(r). \quad (3)$$

Here, $\varepsilon(r)$, $P(r)$, $M(r)$ and $\nu(r)$ represent the radial profile for energy density, pressure, enclosed mass and the metric potential respectively. Complimented with an EoS, the structure Equations (1, 2, 3) are solved numerically to generate the profiles for pressure, energy density, enclosed mass etc. and also the total mass and radius of the star for a given value of central energy density.

Assuming the star is rotating uniformly and the angular velocity (Ω) is sufficiently slow ($\Omega^2 R^3 \ll M$) compared to its Kepler limit, the MoI of a star can be calculated in the slow-rotation approximation using Hartle's prescription (Hartle & Thorne 1968). The metric of a slowly, uniformly rotating star can be expressed at the first order of spin frequency Ω as,

$$ds^2 = -e^{2\nu(r)} dt^2 + e^{2\lambda(r)} dr^2 - 2\omega(r)r^2 \sin^2\theta d\phi dt + r^2 d\theta^2 + r^2 \sin^2\theta d\phi^2, \quad (4)$$

where, ω is the frame-dragging frequency, which satisfies the following differential equation:

$$\frac{d}{dr} \left(r^4 j(r) \frac{d\bar{\omega}(r)}{dr} \right) + 4r^3 \frac{dj(r)}{dr} \bar{\omega}(r) = 0, \quad (5)$$

where $\bar{\omega}(r) = \Omega - \omega(r)$ and $j(r)$ is defined as

$$j(r) = e^{-(\nu(r)+\lambda(r))} = e^{-\nu(r)} \sqrt{1 - 2GM(r)/r}, \quad (6)$$

for $r \leq R$.

Now, we can compute the MoI of the star solving Equation (5) augmented with the TOV equations as:

$$I_{\text{total}} = \frac{8\pi}{3} \int_0^R dr r^4 \frac{(\varepsilon(r) + P(r))}{\sqrt{1 - 2GM(r)/r}} \frac{\bar{\omega}(r)}{\Omega} e^{-\nu(r)}. \quad (7)$$

To calculate the FMI which is responsible for a glitch, we also calculate the crustal contribution to the MoI separately by performing the integration in Equation (7) from the crust-core transition radius to the surface of the star:

$$I_{\text{crust}} = \frac{8\pi}{3} \int_{R_c}^R dr r^4 \frac{(\varepsilon(r) + P(r))}{\sqrt{1 - 2GM(r)/r}} \frac{\bar{\omega}(r)}{\Omega} e^{-\nu(r)} \quad (8)$$

where R_c denotes the crust-core boundary. Note that I_{crust} consists of both the non-superfluid and the pinned superfluid component of the MoI of crust. Thus, I_{crust} cannot be directly related to FMI using the measurements of observed fractional spin-up during a glitch. We provide a prescription for comparing this theoretical estimate with observations in the next section.

4. INTERPRETING THE DATA

The pulsed emission in radio waveband is a direct measure of rotation of the crust of the pulsar, which can be very precisely modeled using the pulsar timing technique. In pulsar timing, predictions of pulse times-of-arrival (TOAs) from a rotational model of the star are compared with the observed TOAs. The difference between the observed and predicted TOAs are called timing residuals, which are minimized in a least-square sense to improve the parameters of the rotational model, thus precisely estimating the time evolution of the rotation of the pulsar. The pre and post glitch models shows a sudden jump in the rotation period ν . The fractional change in ν is therefore available from observations.

If we assume that the spin-up is due to the transfer of angular momentum from a superfluid, which is not co-rotating with the crust, then the fractional MoI of this superfluid to the MoI of the rest of the star for each glitch is given by (Eya et al. 2017)

$$\frac{I_{\text{crsf}}}{I_{\text{rest}}} = -\frac{1}{\dot{\nu}_c} \frac{\Delta\nu_i}{t_i} \quad (9)$$

where I_{crsf} , I_{rest} , $\Delta\nu_i$, $\dot{\nu}_c$ and t_i are the MoI of the pinned crustal superfluid (not co-rotating with the crust), the MoI of the rest of the star (assumed co-rotating with the crust), the spin-up at the i^{th} glitch, the mean rotational spin-down rate and the time elapsed before the i^{th} glitch since the preceding glitch, respectively.

The above equation can be simplified as

$$\frac{I_{\text{crsf}}}{I_{\text{rest}}} = 2\tau_c \left(\frac{\Delta\nu}{\nu} \right)_i \frac{1}{t_i} \quad (10)$$

where $\tau_c (= -\nu/2\dot{\nu}_c)$ is the characteristic age of the pulsar. Since t_i is the time preceding the last glitch, one cannot calculate the $I_{\text{crsf}}/I_{\text{rest}}$ for the first glitch. We want to connect this $I_{\text{crsf}}/I_{\text{rest}}$ with $I_{\text{crust}}/I_{\text{total}}$. Assuming no contribution in the angular momentum transfer from the core superfluid we have,

$$\frac{I_{\text{crust}}}{I_{\text{total}}} = \frac{I_{\text{crsf}} + I_{\text{crnsf}}}{I_{\text{crsf}} + I_{\text{rest}}} > \frac{1}{1 + I_{\text{rest}}/I_{\text{crsf}}}$$

where, I_{crnsf} is the non-superfluid (and hence co-rotating with the crust) component of crustal MoI. Now, since $I_{\text{rest}} \gg I_{\text{crsf}}$, we have $I_{\text{crust}}/I_{\text{total}} > I_{\text{crsf}}/I_{\text{rest}}$ and we can write using Eq. (10):

$$\frac{I_{\text{crust}}}{I_{\text{total}}} > 2\tau_c \frac{1}{t_i} \left(\frac{\Delta\nu}{\nu} \right)_i, \quad (11)$$

This connects our theoretical estimate of FMI with that inferred from observations and this equation has been

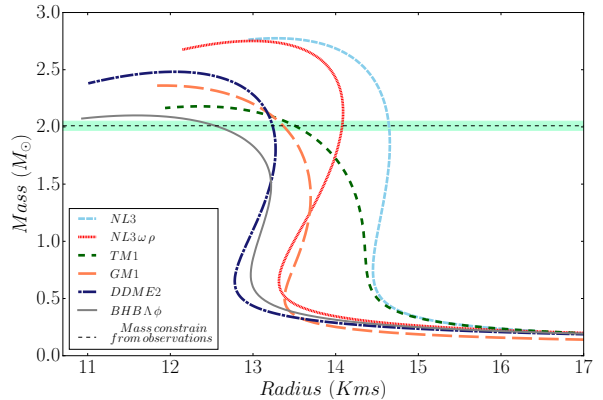


Figure 1. The mass radius diagram for NL3 (sky blue), NL3 $\omega\rho$ (red), TM1 (green), GM1 (orange), DDME2 (dark blue) and BHBA ϕ (grey) EoS. The blue dotted line represents the mass constrain of $2.01 \pm 0.04 M_{\odot}$ from observation (Antoniadis et al. 2013).

used in the next section to produce the histograms estimating the $I_{\text{crust}}/I_{\text{total}}$.

When the entrainment coupling between the neutron superfluid and the crustal non-superfluid component is taken into consideration, we get (Andersson et al. 2012)

$$\frac{I_{\text{crust}}}{I_{\text{total}}} > 2\tau_c \frac{\langle m_n^* \rangle}{m_n} \frac{1}{t_i} \left(\frac{\Delta\nu}{\nu} \right)_i, \quad (12)$$

where $\frac{\langle m_n^* \rangle}{m_n}$ is the ratio of average effective mass of neutrons in the inner crust and of bare neutron mass and has value in the range 4.3 – 5.1 due to the entrainment effect (Chamel 2012; Andersson et al. 2012; Delsate et al. 2016).

5. RESULTS

We have used six different unified equations of state NL3, NL3 $\omega\rho$, GM1, TM1, DDME2 and BHBA ϕ as described in Section 2. The mass radius sequences of these six EoSs are shown in Figure 1. All these EoSs satisfy the present observational constraint on the neutron star maximum mass ($2.01 \pm 0.04 M_{\odot}$) (Antoniadis et al. 2013). It is to be noted that color code to represent various EoSs in Figure 1 has been uniformly applied in all the diagrams throughout the paper.

We have calculated the fraction of MoI of the crust to the total MoI as a function of mass of the stars in percent for each of the six EoSs using Equations (7) and (8) and the results are shown as percentage in the left panel of Figure 2. The distance of the crust-core boundary from the center of the star (R_c) as well as the radius of the star for each EoS are obtained from the solution of TOV equation. Hence, one can readily calculate the crust thickness as $\Delta R = R - R_c$. The right panel of

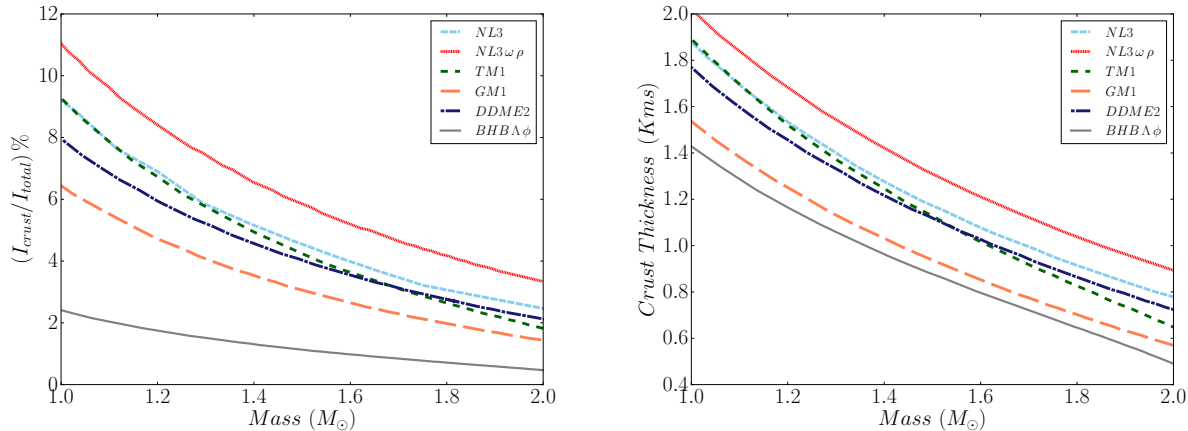


Figure 2. (Left) The fraction of MoI of the crust as compared to the total MoI (expressed in percentage) for six different EoS as a function of stellar mass. (Right) The crust thickness in kilometers as a function of stellar mass.

Figure 2 shows the crust thickness as a function of the stellar mass. It can be clearly seen that the thickness of the crust can be very large $\sim (1.4 - 1.8)$ km for a lighter star of mass $\sim 1 M_{\odot}$ whereas, for massive stars of mass $\sim 2 M_{\odot}$ it can be as small as ~ 0.5 km. Observing the Figure 2, it is very much evident that the relation of the crust thickness and its FMI with the stellar mass go hand in hand. Instead of unified EoS if a polytropic EoS is used for the inner crust as done by Piekarewicz et al. (2014), we find that depending on the choice of the polytropic index the value of FMI gets overestimated by 0 – 8% for a $1.4 M_{\odot}$ NS for NL3 $\omega\rho$ EoS and the error is more for low mass stars. Similar results are expected for other EoSs as well.

The values of FMI estimated from all the observed glitches cataloged so far (Espinoza et al. 2011) are shown in Figure 3, where the distribution of $\log_{10}(\frac{I_{\text{crust}}}{I_{\text{total}}})$, estimated using eq. (11) for all observed glitches, are plotted for different assumed masses of the NS (1.0, 1.2, 1.4, 1.6, 1.8 and $2.0 M_{\odot}$ respectively). The error bars given on each bins are Poissonian error bars. The vertical lines are constraints from our theoretical calculations of $\log_{10}(\frac{I_{\text{crust}}}{I_{\text{total}}})$ for six EoSs considered in this work. We note that the observed $I_{\text{crust}}/I_{\text{total}}$ always overestimates the superfluid reservoir as it assumes the crust is made entirely of pinned superfluid. Hence, the actual contribution from the superfluid in the crust towards glitch is smaller than the estimated $I_{\text{crust}}/I_{\text{total}}$. In all the cases, the NL3 $\omega\rho$ model can explain a larger FMI as it has the largest crust (Fig. 2). It is evident that there is a significant fraction of the glitch events, which cannot be explained solely by the crustal superfluidity. The number of such events (out of 335 glitches), which cannot be explained by the crustal superfluidity alone for all six EoSs and six different assumed NS masses are

tabulated in Table 1. The estimate of $\log_{10}(\frac{I_{\text{crust}}}{I_{\text{total}}})$ considering entrainment are also plotted in the same figure. As expected, the fraction of glitches, which cannot be explained entirely by the crustal superfluidity alone is larger in presence of entrainment.

From the Table 1, we can clearly conclude that at least 1 to 20 % glitch events without entrainment require the angular momentum reservoir of pinned superfluid located outside the crust, even in the limiting case of the crust entirely made up of pinned superfluid. When the entrainment is taken into account the percentage changes to 4 % to 36 %. Therefore, we must consider the possibility of the contribution of the core in these glitch events.

6. CONCLUSIONS AND DISCUSSIONS

In this work, a unified treatment of EoS, using a relativistic mean field approach, has been carried out to estimate the fraction of MoI of the crust compared to the total NS MoI. We have used individual glitches instead of the average of glitches defined via activity parameter, in our estimation of FMI. We compared the theoretical estimates with those obtained from observations and conclude that about a few percentage of glitches cannot be explained by angular momentum transfer from the pinned superfluid in the crust alone, even without the entrainment effect. The fraction of such glitches range from 1 to 20 % for different EoSs and assumed NS masses.

In this context, it is important to note that the recent binary neutron star merger event GW170817 has provided unique insights on the global properties of isolated neutron stars (Abbott et al. 2017). Several authors have shown that GW170817 sets an upper limit

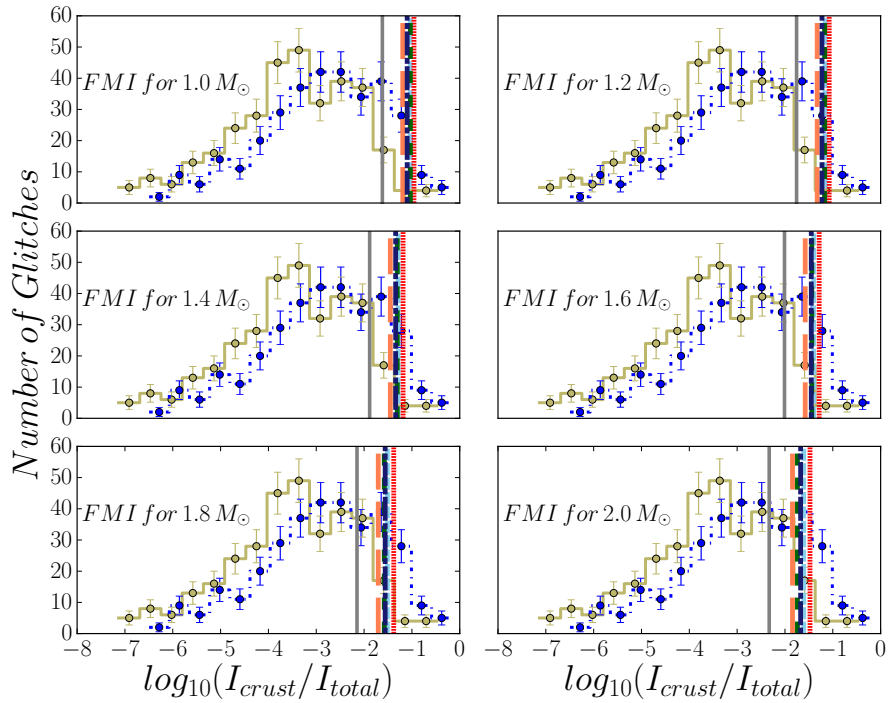


Figure 3. Figure shows the distribution of I_{crust}/I_{total} . The vertical lines in each plot correspond to the fractional moment of inertia for six different equations of state. The plots from top left to bottom right correspond to mass of 1, 1.2, 1.4, 1.6, 1.8 and $2.0 M_{\odot}$ respectively. The distribution plotted with yellow line corresponds to the distribution without entrainment, whereas the distribution plotted with blue dotted line has been constructed taking entrainment value $\frac{\langle m_n^* \rangle}{m_n} = 4.35$ into account. Both distribution are obtained from 335 glitches.

*	$1.0 M_{\odot}$	$1.2 M_{\odot}$	$1.4 M_{\odot}$	$1.6 M_{\odot}$	$1.8 M_{\odot}$	$2.0 M_{\odot}$
NL3	4(16)	5(22)	8(31)	8(39)	11(71)	13(60)
NL3 $\omega\rho$	4(12)	5(17)	5(25)	8(31)	8(37)	11(47)
DDME2	5(17)	7(28)	8(34)	10(43)	13(56)	16(66)
TM1	4(16)	5(23)	8(32)	10(43)	13(56)	18(70)
GM1	5(25)	8(33)	10(43)	13(56)	17(68)	28(80)
BHBA ϕ	14(61)	21(71)	31(81)	37(94)	53(106)	68(121)

Table 1. Table shows the number of glitch events that cannot be explained from crustal superfluid alone. The quantities in parenthesis shows glitch event when entrainment ($\frac{\langle m_n^* \rangle}{m_n} = 4.35$) is taken into account for six different assumed NS masses (columns) and six different EoSs (rows).

of $\sim 2.1 - 2.2M_{\odot}$ on the maximum mass of a NS (Margalit & Metzger 2017; Shibata et al. 2017; Rezzolla et al. 2018; Ruiz et al. 2018). The radius of a $1.4M_{\odot}$ star has also been constrained to $\lesssim 13.5$ km (Most et al. 2018; Abbott et al. 2018; Nandi & Char 2018). In this paper, we have used both stiff EoS (NL3) and moderately soft EoS (BHBA ϕ) for representative purpose. It is evident from Figs 1 and 2 that stiffer EoS, like NL3, usually leads to a larger radius. This makes the crustal thickness as well as the I_{crust}/I_{total} larger than that of a moderately softer EoS. While a majority of glitches can be

explained by transfer of angular momentum from crustal superfluid for such stiffer EoS, some glitches still remain unexplained. On the other hand, a larger number of glitches are inconsistent with the transfer of angular momentum solely from crustal superfluid for a moderately softer EoS, such as BHBA ϕ , which predict a maximum mass and radius consistent with the upper limit from GW170817 unlike stiffer EoS (Bhat & Bandyopadhyay 2018). Therefore, the conclusion that only crustal contribution to the angular momentum transfer can not ac-

count for all the glitches becomes stronger if the constraints from GW170817 are taken into account.

The number of unexplained glitches is even larger if entrainment effect is taken into consideration, as expected. It is worth mentioning here that a recent study (Watanabe & Pethick 2017) showed that the effect of entrainment is not that significant, as estimated earlier (Chamel 2012). Thus, our calculations suggests that the superfluid in the core is also likely to participate at least in the larger glitches. The rotation of crustal superfluid is believed to be constrained due to pinning of vortex to the nuclei in the crustal lattice, thus conserving the areal density of vortices (Sauls 1989). In order for the superfluid in other parts of the star, particularly the core, to participate in a glitch, similar constraint is required on this fraction of superfluid, which was generally believed to co-rotate with the crust and slows down in synchronism by expelling vortices. Our analysis also confirms the presence of extra angular momentum reservoir along with the NS crust.

For a glitch to happen in the star, it is essential to pin superfluid vortices to some structures, which can co-rotate with the stellar crusts. One such possibility is presence of mixed state at certain depth of the stellar core. The region is marked by presence of confined (hadronic) and de-confined (quark) matter co-existing in equilibrium. The energetics of such region forces the non-dominating component to form crystal structures of various shapes evolving with the density. They could be a potential zone of extra angular momentum reservoir (Glendenning 2000). Similar kind of crystalline structure can also form due to a mixed phase of kaon condensates inside nuclear matter as a first order phase transition (Glendenning & Schaffner-Bielich 1999). The other possible way of pinning could be between Abrikosov fluxoids along the magnetic moment due to presence of paired proton superconductor (Sauls 1989; Ho et al. 2017) at the core of the NS with Onsagar-Feynman vortices along the rotation axis (Bhattacharya & Srinivasan 1995). This novel mechanism of inter-pinning between fluxoids and vortices were used in literature to expel the magnetic fluxoids from core to the crust of star via the spinning down of the NS. But this mechanism may not probably help in building up of angular momentum,

which can be expelled at once to produce a sudden jump in angular velocity as observed in glitches.

Recently, Gügercinoğlu & Alpar (2014) have suggested pinning of superfluid in outer core by a toroidal field similar to pinning of crustal superfluid with a FMI of superfluid associated with this toroidal magnetic field (I_{tor}/I_{total}) of the order of $0.3-1.2 \times 10^{-2}$ (Gügercinoğlu 2017). This presents an attractive alternative for contribution from superfluid in outer core mediated by magnetic field as a source of extra MoI reservoir for glitches not explained by crustal superfluid. Large glitches in PSR B2334+61 and J1718-3718 could be explained by this mechanism (Gügercinoğlu & Alpar 2016). It may be noted that a small fraction of core MoI is needed to explain larger FMIs in our sample as expected, considering the fraction of core superfluid associated with this toroidal magnetic field to be much smaller than total MoI of core. Thus, this mechanism can potentially explain the glitches in our study, where the crustal superfluid is not enough.

Interestingly, in pulsars, such as PSR B0833-45, B1046-58, B1338-62 and B1737-30, we see both small and large glitches. The glitch size varies by a factor of 258, 160, 236 and 3811 in these pulsars respectively. Our calculations suggest that in all these pulsars atleast one glitch event cannot be explained by BHBA ϕ EoS, whereas other EoSs used can explain the glitches from the crustal angular momentum reservoir except for PSR B1046-58. In case of PSR B1046-58 the glitch which had $I_{crust}/I_{total} = 33\%$, cannot be explained by any of the EoSs used taking even $1.0 M_{\odot}$ as the fiducial mass of the NS. Thus, we conclude at least some of the glitches require a participation of core, whereas the smaller glitches can be caused by the crust alone. This also may provide a probe for the strength of a coupling agent and the angular momentum transfer mechanism from core to the crust of the star. Future theoretical calculations to probe this aspect are motivated from this work .

ACKNOWLEDGEMENTS

We would like to thank H. Pais for kindly providing us the EoS table for the GM1 inner crust. P. Char acknowledges support from the Navajbai Ratan Tata Trust. BCJ acknowledge support for this work from DST-SERB grant EMR/2015/000515.

REFERENCES

Abbott, B. P. *et al.* (LIGO Scientific and Virgo Collaborations) 2017, PhRvL, 119, 161101

Abbott, B. P. *et al.* (LIGO Scientific and Virgo Collaborations) 2018, arXiv:1805.11581

- Alpar, M. A., Nandkumar, R., & Pines, D. 1985, ApJ, 288, 191
- Alpar, M. A., Langer, S. A., & Sauls, J. A. 1984, ApJ, 282, 533
- Alpar, M. A., Pines, D., Anderson, P. W., & Shaham, J. 1984, ApJ, 276, 325
- Alpar, M. A., Chau, H. F., Cheng, K. S., & Pines, D. 1993, ApJ, 409, 345
- Andersson N., Glampedakis K., Ho W.C.G., & Espinoza C. M., 2012, PhRvL, 109, 241103
- Antoniadis, J., Freire, P. C. C., Wex, N., et al. 2013, Science, 340, 448
- Baldo, M., Saperstein, E.E., & Tolokonnikov, S.V. 2005, NuPhA, 749, 42.
- Banik, S., Hempel M., & Bandyopadhyay D. 2014, ApJS, 214, 22.
- Baym, G. Pethick C., & Sutherland P. 1971, ApJ, 45, 429.
- Baym G., Bethe H. A., & Pethick C. J. 1971, NuPhA, 175, 225.
- Bhat S. A., & Bandyopadhyay D., arXiv:1807.06437 [astro-ph.HE].
- Bhattacharya, D., & Srinivasan, G. 1995, *X-ray Binaries*, 495 (Cambridge University Press)
- Chamel, N., & Haensel, P. 2008, Living Rev. Relativ., 11, 10
- Chamel N., 2012, PhRvC, 85, 035801
- Chamel N. 2013, PhRvL, 110, 011101.
- Datta, B., & Alpar, M. A. 1993, A&A, 275, 210
- Delsate T., Chamel N., Grlebeck N., Fantina A. F., Pearson J. M., & Ducoin C. 2016, PhRvD, 94, 023008.
- Dutra, M., Lourenço, O., Avancini, S. S., et al. 2014, PhRvC, 90, 055203.
- Epstein, R. I., & Baym, G. 1988, ApJ, 328, 680.
- Espinoza, C. M., Lyne, A. G., Stappers, B. W., & Kramer, M. 2011, MNRAS, 414, 1679, <http://www.jb.man.ac.uk/pulsar/glitches.html>.
- Eya, I. O., Urama, J. O., & Chukwude, A. E. 2017, ApJ, 840, 56
- Fuentes, J. R., Espinoza, C. M., Reisenegger, A., et al. 2017, A&A, 608, A131
- Fortin M., Raduta Ad. R., Gulminelli F., Zdunik J. L., Haensel P. & Bejger M., 2016, PhRvC, 94, 035804
- Fattoyev F. J., Piekarewicz J., & Horowitz C. J. 2018, PhRvL, 120, 172702.
- Gügercinoğlu, E., & Alpar, M. A. 2014, ApJL, 788, L11
- Gügercinoğlu, E., & Alpar, M. A. 2016, MNRAS, 462, 1453
- Gügercinoğlu, E. 2017, MNRAS, 469, 2313
- Glendenning N. K., Schaffner-Bielich, J., 1999, PhRvC, 60, 025803
- Glendenning N. K., 2000, *Compact Stars, Nuclear Physics, Particle Physics, and General Relativity*, 2nd ed. (Springer-Verlag, New York).
- Ginzburg, V.L., & Kirzhnits, D.A. 1964, Zh. Eksp. Teor. Fiz., 47, 2006.
- Grill F., Pais H., Providência C., & Vidaña I., 2014, PhRvC, 90, 045803
- Haensel, P. 2001, Physics of Neutron Star Interiors, 578, 127.
- Haensel P., Potekhin A. Y., & Yakovlev D. G., 2007, *Neutron Stars 1, Equation of State and Structure*, (Springer).
- Hartle J. B., & Thorne K. S. 1968, ApJ, 153, 807
- Haskell, B., & Melatos, A. 2015, Int. J. Mod. Phys. D, 24, 1530008
- Ho, W. C. G., Espinoza, C. M., Antonopoulou, D., & Andersson, N. 2015, Science Advances, 1, e1500578
- Ho, W. C. G., Andersson, N., & Graber, V. 2017, PhRvC, 96, 065801
- Horowitz C. J., & Piekarewicz J., 2001, PhRvL, 86, 5647; 2001, PhRvC, 64, 062802
- Krawczyk, A., Lyne, A. G., Gil, J. A., & Joshi, B. C. 2003, MNRAS, 340, 1087
- Lalazisis G. A., König J., & Ring P., 1997, PhRvC, 55, 540
- Lalazisis G. A., Niksic T., Vretenar D. & Ring P., 2005, PhRvC, 71, 024312
- Li, A., Dong, J. M., Wang, J. B., & Xu, R. X. 2016, ApJS, 223, 16
- Link, B., Epstein, R. I., & van Riper, K. A. 1992, Nature, 359, 616
- Link, B., Epstein, R. I., & Lattimer, J. M. 1999, PhRvL, 83, 3362
- Lyne, A. G. 1992, Philosophical Transactions of the Royal Society of London Series A, 341, 29
- Lyne, A. G. 1996, IAU Colloq. 160: Pulsars: Problems and Progress, 105, 73
- Lyne, A. G., Shemar, S. L., & Smith, F. G. 2000, MNRAS, 315, 534
- Margalit, B. & Metzger, B. D. 2017, ApJL, 850, L19
- Manchester, R. N., & Hobbs, G. 2011, ApJL, 736, L31
- Most, E. R., Weih, L. R., Rezzolla, L., & Schaffner-Bielich, J. 2018, PhRvL, 120, 261103
- Radhakrishnan, V., & Manchester, R. N. 1969, Nature, 222, 228
- Nandi R., & Bandyopadhyay D. 2011, J. Phys. Conf. Ser., 312, 042016.
- Nandi R., Bandyopadhyay D., Mishustin I. & Greiner W. 2011, ApJ, 736, 156.
- Nandi R., & Char P. 2018, ApJ, 857, 12.
- Negele J. W., & Vautherin D. 1973, NuPhA, 207, 298.

- Oertel M., Hempel M., Klähn T., & Typel S., 2017, *Rev. Mod. Phys.*, 89, 015007
- Page D., & Reddy S. 2006, *Annu. Rev. Nucl. Part. Sci.* 56, 327.
- Piekarewicz J., Fattoyev F. J., & Horowitz C. J. 2014, *PhRvC*, 90, 015803.
- Pizzochero, P. M., Antonelli, M., Haskell, B., & Seveso, S. 2017, *Nat. Astron.*, 1, 0134
- Read J. S., Benjamin D. L., Owen, B. J., & Friedman J. L. 2009, *PhRvD*, 79, 124032.
- Rezzolla, L., Most, E. R., & Weih, L. R. 2018, *ApJL*, 852, L25
- Ruiz, M., Shapiro, S. L. & Tsokaros, A. 2018, *PhRvD*, 97, 021501(R)
- Rüster S. B., Hempel, M., & Schaffner-Bielich J. 2006, *PhRvC*, 73, 035804.
- Sauls, J. 1989, *NATO Advanced Science Institutes (ASI) Series C*, 262, 457.
- Sedrakian, A., & Clark, J. W. 2006, *Pairing in Fermionic Systems: Basic Concepts and Modern Applications*, 8, 135.
- Shemar, S. L., & Lyne, A. G. 1996, *MNRAS*, 282, 677
- Shibata, M., Fujibayashi, S., Hotokezaka, K., Kiuchi, K., Kyutoku, K., Sekiguchi, Y., & Tanaka, M. 2017, *PhRvD*, 96, 123012
- Sugahara Y., & Toki H., 1994, *NuPhA*, 579, 557
- Wang, N., Manchester, R. N., Pace, R. T., et al. 2000, *MNRAS*, 317, 843
- Watanabe G., & Pethick C. J. 2017, *PhRvL*, 119, 062701.
- Yu, M., Manchester, R. N., Hobbs, G., et al. 2013, *MNRAS*, 429, 688